International Journal of Nanomedicine

Dovepress
open access to scientific and medical research

Open Access Full Text Article

ORIGINAL RESEARCH

Bioinspired Nanofiber Scaffold for Differentiating Bone Marrow-Derived Neural Stem Cells to Oligodendrocyte-Like Cells: Design, Fabrication, and Characterization

This article was published in the following Dove Press journal:
International Journal of Nanomedicine

Fatemeh Rasti Boroojeni[1,2]
Shohreh Mashayekhan[1]
Hojjat-Allah Abbaszadeh[3,4]
Mohamadhasan Ansarizadeh[1,5]
Maryam-Sadat Khoramgah[4]
Vafa Rahimi Movaghar[6]

[1]Department of Chemical and Petroleum Engineering, Sharif University of Technology, Tehran, Iran; [2]Division of Molecular Physics, Department of Physics, Chemistry and Biology, Linköping University, Linköping, Sweden; [3]Hearing Disorders Research Center, Loghman Hakim Hospital, Shahid Beheshti University of Medical Sciences, Tehran, Iran; [4]Laser Application in Medical Sciences Research Center, Shahid Beheshti University of Medical Sciences, Tehran, Iran; [5]Biocenter Oulu, Faculty of Biochemistry and Molecular Medicine, University of Oulu, Oulu, Finland; [6]Sina Trauma and Surgery Research Center, Tehran University of Medical Sciences, Tehran, Iran

Correspondence: Hojjat-Allah Abbaszadeh
Hearing Disorders Research Center, Loghman Hakim Hospital, Shahid Beheshti University of Medical Sciences, PO Box: 19395-4719, Tehran, Iran
Tel/Fax +98 21-22439976
Email Dr.Abbaszadeh@sbmu.ac.ir

Vafa Rahimi Movaghar
Sina Trauma and Surgery Research Center, Tehran University of Medical Sciences, Tehran, Iran
Tel +98 21-66757001
Fax +98 21-66757009
Email V_rahimi@sina.tums.ac.ir

Background: Researchers are trying to study the mechanism of neural stem cells (NSCs) differentiation to oligodendrocyte-like cells (OLCs) as well as to enhance the selective differentiation of NSCs to oligodendrocytes. However, the limitation in nerve tissue accessibility to isolate the NSCs as well as their differentiation toward oligodendrocytes is still challenging.

Purpose: In the present study, a hybrid polycaprolactone (PCL)-gelatin nanofiber scaffold mimicking the native extracellular matrix and axon morphology to direct the differentiation of bone marrow-derived NSCs to OLCs was introduced.

Materials and Methods: In order to achieve a sustained release of T3, this factor was encapsulated within chitosan nanoparticles and chitosan-loaded T3 was incorporated within PCL nanofibers. Polyaniline graphene (PAG) nanocomposite was incorporated within gelatin nanofibers to endow the scaffold with conductive properties, which resemble the conductive behavior of axons. Biodegradation, water contact angle measurements, and scanning electron microscopy (SEM) observations as well as conductivity tests were used to evaluate the properties of the prepared scaffold. The concentration of PAG and T3-loaded chitosan NPs in nanofibers were optimized by examining the proliferation of cultured bone marrow-derived mesenchymal stem cells (BMSCs) on the scaffolds. The differentiation of BMSCs-derived NSCs cultured on the fabricated scaffolds into OLCs was analyzed by evaluating the expression of oligodendrocyte markers using immunofluorescence (ICC), RT-PCR and flowcytometric assays.

Results: Incorporating 2% PAG proved to have superior cell support and proliferation while guaranteeing electrical conductivity of 10.8×10^{-5} S/cm. Moreover, the scaffold containing 2% of T3-loaded chitosan NPs was considered to be the most biocompatible samples. Result of ICC, RT-PCR and flow cytometry showed high expression of O4, Olig2, platelet-derived growth factor receptor-alpha (PDGFR-α), O1, myelin/oligodendrocyte glycoprotein (MOG) and myelin basic protein (MBP) high expressed but low expression of glial fibrillary acidic protein (GFAP).

Conclusion: Considering surface topography, biocompatibility, electrical conductivity and gene expression, the hybrid PCL/gelatin scaffold with the controlled release of T3 may be considered as a promising candidate to be used as an in vitro model to study patient-derived oligodendrocytes by isolating patient's BMSCs in pathological conditions such as diseases or injuries. Moreover, the resulted oligodendrocytes can be used as a desirable source for transplanting in patients.

Keywords: nanofibers scaffold, oligodendrocyte cells, controlled triiodothyronine release, central nervous system, polyaniline graphene

submit your manuscript | www.dovepress.com
DovePress
http://doi.org/10.2147/IJN.S248509

Introduction

The aim of tissue engineering and regenerative medicine is to speed up the healing process of the damaged tissue and to promote regeneration of new tissue after injury.[1] In general, the damage to the central nervous system (CNS) results in axonal damage and myelin degradation.[2] In addition, oligodendrocyte responsible for myelination in CNS also will be damaged, which causes more axonal dieback known as secondary damages.[3] The damage to CNS causes hyperactivation of astrocyte cells which leads to the secretion of proteoglycans including chondroitin sulfate, known to be a potent inhibitor of axonal growth. Additionally, glial scar tissue hinders axonal growth by creating physical and chemical barriers.[4] In order to repair the CNS, the selective differentiation of NSCs into neurons and OLCs is crucial, while the differentiation to astrocytes is not desirable.[5] The goal of all regenerative strategies in the CNS is to modulate the activity of astrocytes and increase the regrowth of damaged axons as well as oligodendrocytes.[4] Biomimicking the CNS microenvironment is crucial because CNS development is highly dependent on chemical and physical factors.[6] In the past, much of the researchers' focus had been devoted to the development of the therapeutic approaches that improved the recovery of neurons. Recently, special attention has been paid to improve myelination and the provision of OLCs in the site of injury.[7] Different strategies have been proposed to differentiate stem cells to OLCs. Although direct use of differentiation factors in cell culture media or using transcription factor-encoding viral vectors as the elementary approaches for differentiating stem cells towards the OLCs were somewhat successful, it is verified that taking advantage of biomaterials and scaffolds will be safer and more efficient than previous approaches.[8]

There are various differentiation factors including retinoic acid, thyroid hormone, and platelet-derived growth factor (PDGF), which have been frequently used to direct the differentiation of NSCs to neurons, and OLCs.[9] Among the hormones affecting the CNS, thyroid hormone plays a crucial role in its function, which affects not only neurons but also the growth and differentiation of neuron-supporting cells.[10] Inspired by the very important role of the thyroid hormone in the CNS and its significant effect on differentiating NSCs into OLCs, T3 as OLCs differentiation factor has been used in the present study.[11] It is predicted that the use of stem cells for repair and regeneration of the spinal cord will have a promising future due to their high proliferation and differentiation potential. However, the problem with using these cells is the targeted differentiation into the desired cell line.[12] Among different types of stem cells, BMSCs have special characteristics that regulate the environment of the CNS and ultimately lead to axon reconstruction and motor recovery.[13] Therefore, BMSCs would be desirable as a source of either autograft or allograft cells for transplanting into the CNS due to their special characteristics such as availability, low immunogenicity, high growth rate, and the ability to differentiate to glial cells to treat diseases related to the CNS.[11] Till now, a wide range of scaffolds have been fabricated to be used in the regeneration of the CNS and spinal cord, each of which has its own advantages and disadvantages.[3,8] However, the design and fabrication of a bioactive scaffold that supports OLCs differentiation and proliferation are valuable. To stimulate OLCs differentiation by using the scaffold to mimic its natural microenvironment, the scaffold should have desired structural and morphological characteristics similar to the native axons. Considering the porosity and fibrous structure, electrospun scaffolds resemble the neural extracellular matrix. In addition, they may support adhesion, proliferation, and differentiation of various cell types due to the high surface-to-volume ratio.[14] Moreover, in order to resemble the oligodendrocyte microenvironment, electrical conductivity should be taken into account.[15] Among different types of conductive materials, a small amount of polyaniline combined with graphene nanosheets denoted as PAG is considered to be a biocompatible material, which increase the electrical conductivity efficiently. These PAG previously synthesized and characterized by Baniasdi et al were used in this study to increase the electrical conductivity of the scaffold.[16]

It has been shown that chitosan NPs can be a very good candidate as a carrier for drug or differentiation factor. The benefit of controlled release of various factors encapsulated in chitosan NPs-loaded nanofibers has already been reported in several studies.[17,18] Moghadasi Boroujeni et al showed that the encapsulation of TGF-β1 in chitosan NPs-loaded nanofibers resulted in significant enhancement of human Wharton's Jelly-derived mesenchymal stem cell's differentiation toward myogenic lineage, compared with bolus delivery of TGF-β1.[18] In a recent work reported by our group, the encapsulation of dexamethasone (DEXP) in chitosan NPs, as an inhibitor of astrocyte proliferation, reduced the burst release of DEXP from PCL/gelatin

nanofiber scaffold and caused a sustained release of this factor.[19] In the present study, chitosan NPs have been used as a carrier to encapsulate T3 as OLCs differentiation factor. In summary, the main purpose of this study was to design and fabricate a conductive nanofibrous scaffold with controlled release of T3 to differentiate BMSCs-derived NSCs to OLCs. In our previous study, it was showed that the synergistic effect of scaffold topography and the sustained release of differentiating factor resulted in improved efficiency of cell differentiation.[18] In this study, the synergistic effect of the scaffold conductivity and sustained release of T3 was investigated on NSCs differentiation toward OLCs. The conductive scaffold consists of biodegradable and biocompatible gelatin, PCL, T3-containing loaded chitosan NPs, and PAG. Dual-electrospinning technique was utilized to fabricate nanofibers. PCL solution containing T3-loaded chitosan NPs and gelatin solution containing PAG were electrospinned on different sides of the collector simultaneously. First, the effect of PAG nanoparticles on scaffold characteristics and cell viability were analyzed, and then the effect of T3-loaded chitosan NPs on the scaffold and the differentiation were studied. The graphical abstract of this work is illustrated in Figure 1. As it is shown, BMSCs were isolated from adult rats and transdifferentiated into neurospheres (NSFs), which was followed by the differentiation of NSFs into NSCs. Next, NSCs were seeded on the fabricated scaffold in order to induce differentiation towards OLCs. To evaluate the differentiation of NSCs to OLCs, the expression of platelet-derived growth factor receptor-alpha (PDGFR-α), Olig 2, O4, O1, myelin/oligodendrocyte glycoprotein (MOG), and myelin basic protein (MBP) were analyzed. It has been reported that early oligodendrocyte progenitors express PDGFR-α, while late oligodendrocyte progenitors and pre oligodendrocytes express Olig 2 and O4[11,20]. The expression of O1 and MOG as well as MBP will be upregulated by immature oligodendrocyte and mature oligodendrocyte, respectively.[11] In addition, the expression of the glial fibrillary acidic protein (GFAP) as an astrocyte marker was analyzed to evaluate the selective differentiation of NSCs to oligodendrocytes.[8]

Materials and Methods

Materials

Poly-ε-caprolactone (PCL, Mw = 80 KDa), gelatin (from porcine skin), chloroform, MTT (3[4,5- dimethylthiazol-2-yl]-2,5-diphenyltetrazolium bromide), tripolyphosphate

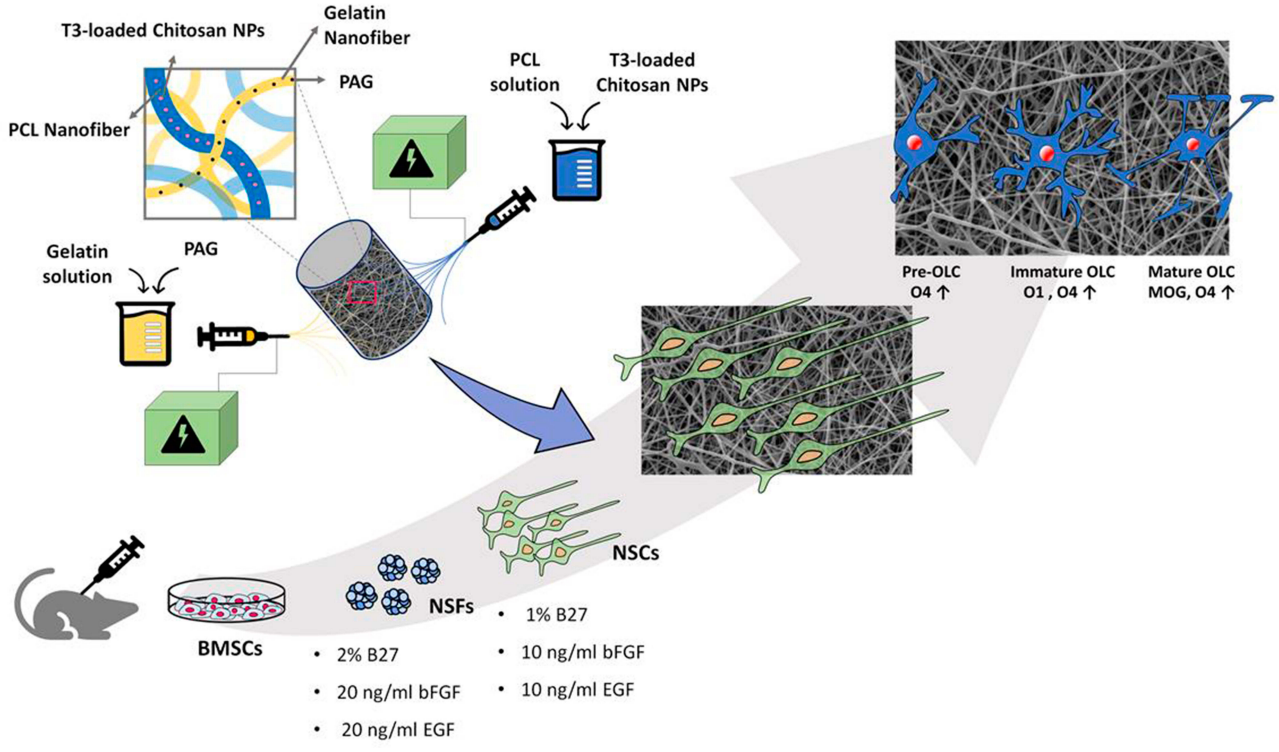

Figure 1 Schematic illustration of cell preparation and scaffold fabrication.

(TPP), chitosan (medium molecular weight), platelet-derived growth factor (PDGF), heregulin, basic fibroblast growth factor (bFGF), ethidium bromide, and triiodothyronine were all purchased from Sigma-Aldrich. Dimethyl formamide (DMF), acetic acid and glutaraldehyde were supplied by Merck. Dulbecco's Modified Eagle's medium (DMEM, high glucose), fetal bovine serum (FBS), trypsin/EDTA, trypan blue stain (0.4 %) and phosphate buffer saline (PBS) were provided by Bio-Idea group. Triiodothyronine ELIZA kit was purchased from Pishtaz Teb Zaman Diagnostics Company. CD34, CD45, CD90, CD44, Nestin, NF68, GFAP antibodies all purchased from Chemicon, USA. The RNX-Plus Kit, DNase I, and strand cDNA Synthesis Kit were purchased from Thermo Fisher Scientific. Mouse anti-O4 monoclonal antibody, FITC conjugated rabbit anti-mouse secondary antibody, and mouse anti-O1 monoclonal antibody were provided from EMD Millipore Corporation. Mouse anti-MOG monoclonal antibody was supplied by Covance.

Fabrication of Conductive PAG-Loaded Gelatin Nanofiber Scaffold

In this study to increase the conductivity of nanofibrous scaffold, PAG synthesized by Baniasadi et al[16] was used. The nanoparticles were previously characterized by the same group. First, in order to find the optimal percentage of PAG to prevent cellular toxicity, different amounts of this nanoparticle were added to the gelatin solution, and polycaprolactone PCL solution was electrospun. PCL solution was prepared by adding 0.36 g of PCL in 3 mL of chloroform:DMF (1.8/1.2 mL). The gelatin solution was also prepared by dissolving 2.5 g of gelatin in 4 mL of 40% ($v.v^{-1}$) acetic acid solution and different amount of PAG suspension were added and stirred for 3 h. The final percentage of PAG in the gelatin solution was considered to be 1%, 2% and 3% ($w.v^{-1}$). The dual-electrospinning process was done by means of two different needles on opposite sides of a Nano Model electrospinning device (Tehran, Iran). In order to overcome the surface tensile force and form the jet, positive 16 kV and 20 kV charges were applied to PCL and gelatin solutions, respectively. PCL and gelatin volume flow rates were maintained at 0.5 $mL.h^{-1}$. The optimal operating distance from the needle to the collector was selected to be about 15 cm and 17 cm for gelatin and PCL solutions, respectively. A cylinder collector (33 cm × 17 cm) coated with aluminum foil with a rotational speed of 300 rpm was utilized. At the end of the electrospinning process to allow gelatin nanofibers to coat the surface of scaffold, PCL electrospinning stopped, and only gelatin electrospinning continued for 20 min. It should be noted that all experiments were carried out at temperature between 25°C and 27°C and humidity of 30–35%. The components of fabricated scaffolds are shown in Table 1.

Fabrication of T3-Loaded PCL Nanofiber Scaffold

Chitosan NPs Preparation

In this study, chitosan NPs were synthesized by the ionic gelation method while T3 was encapsulating within the chitosan NPs. First, chitosan was dissolved in 1% $w.v^{-1}$ acetic solution with a concentration of 1.7 $mg.mL^{-1}$ followed by the addition of 1 N NaOH to adjust its pH at 5.5. Besides, the T3 stock solution was achieved by dissolving in 1 N NaOH. The isoelectric point (PI) of chitosan is approximately 6.2, and pK of hydroxyl phenol group of T3 is 8.45. Under these conditions, the pH of the chitosan was below PI, and consequently had a positive charge.[21] TPP solution (0.45 $mg.mL^{-1}$), an anionic cross-linking agent, was used to form chitosan NPs. The pH of the TPP solution was adjusted to 10. Given that the pK of the phenolic hydroxyl group of T3 is about 8.45, the T3 solution was added to the TPP solution in order to enhance the ionization of the hydroxyl group and increase its negative charge. Then, 12 mL TPP solution containing T3 was added to 30 mL chitosan solution followed by stirring for 1 h at room temperature to form nanoparticles. The weight ratio of chitosan to T3 was fixed at 1:100. After the formation of nanoparticles, they were collected by ultracentrifuging at 24,000 rpm for 60 min. Eventually, nanoparticles were washed with water and dispersed in DMF containing 2% ($v.v^{-1}$) and Tween 80 using a homogenizer.

Size Distribution and Morphology of Chitosan NPs

The size distribution of T3-loaded chitosan NPs in terms of the number was obtained by using a dynamic light

Table 1 Experimental Groups for Conductive Scaffold Fabrication with Varied PAG Content

Sample	Condition
PG	PCL/gelatin scaffold without PAG and without chitosan NPs
PG/PAG 1	PCL/gelatin scaffold containing 1% PAG
PG/PAG 2	PCL/gelatin scaffold containing 2% PAG
PG/PAG 3	PCL/gelatin scaffold containing 3% PAG

scattering (DLS) method. Zetasizer Nano S (Red badge-Malvern Instruments, UK) was used to determine the size and distribution of loaded chitosan NPs. Field-emission scanning electron microscope (FESEM, Tescan, Mira III, Czechia) operating at 15 kV was used to analysis the morphology of dried nanoparticles after gold coating.

Electrospinning of T3-Loaded PCL Nanofiber Scaffold

The process of electrospinning T3-loaded nanofiber scaffold was similar to what mentioned before with some modification for PCL nanofibers. In this step PCL nanofibers contained T3-loaded chitosan NPs. In order to prepare a PCL solution containing 1%, 2% and 3% ($w.v^{-1}$) of chitosan NPs, 0.36 g of PCL was poured in 1.8 mL chloroform and different amount of chitosan NPs were suspended in DMF, and finally stirred for 2 h. The electrospinning conditions were the same for both gelatin and PCL nanofibers.

T3 Encapsulation Efficiency and Release Behavior

To determine the encapsulation efficiency (EE) and loading capacity (LC) of T3 in chitosan NPs, the amount of T3 present in supernatant obtained by ultracentrifugation of nanoparticle suspension at 24,000 rpm for 1 h at 4°C was evaluated by ELISA kit. Then, encapsulation efficiency was calculated by the following equation (1).

$$EE\% = \frac{A - B}{A} \times 100 \quad (1)$$

where A is the amount of primary and B is the final concentration of T3 in the supernatant after centrifugation. Loading capacity for chitosan NPs were obtained by the following equation (2).

$$LC = \frac{C}{D} \quad (2)$$

where C is the amount of loaded T3 and D is the amount of chitosan. In order to investigate the release profile of T3 from the scaffold, 100 mg scaffold containing chitosan NPs and PAG were put in 10 mL of PBS (pH = 7.4) in the 6-well plate in shaking incubator at 80 rpm and 37°C. At specific intervals, 4 mL sample was taken from the plate and replaced with 4 mL fresh PBS solution. The concentration of T3 in the PBS solution was then measured using an ELISA kit. The total amount of T3 released from the scaffold at time i shown by M_i is calculated using equation (3).

$$M_i = C_i V + \sum C_{i-1} V_s \quad (3)$$

where C_i is the concentration of the sample taken from release medium at time i. Also, V is the total volume of release medium, and V_s is the sample volume taken at time i.

Scaffold Characterization

Conductivity Measurement

The aim of this test was to investigate the effect of conductive nanoparticles on the conductivity of scaffolds. A homemade 4-point probe resistor device was utilized. The probes were placed simultaneously at 2.5 mm distance from each other on the samples. By applying the voltage to the sample, the electrical current was measured, and the scaffold resistance was obtained by the following equation (4).

$$\text{Conductance} = \frac{\text{Current(A)}}{\text{Voltage(V)}} \quad (4)$$

Biodegradation Rate

To test the biodegradability of scaffolds, they were placed in a vacuum oven for 24 h to become thoroughly dry. Then, the scaffolds were weighed and put in a PBS solution in a shaker incubator at 100 rpm at 37°C. After 7, 14, and 21 days, scaffolds were taken out, washed with distilled water and placed in the vacuum oven for 24 h to become completely dry and then, were weighed. Using Equation (5), the percentage of scaffold weight loss was calculated obtained at any time.[22]

$$\text{Biodegradation rate } (\%) = \frac{W_0 - W_i}{W_0} \times 100 \quad (5)$$

where W_0 and W_i are the weight of scaffold at the beginning and time i, respectively.

Scanning Electron Microscope (SEM)

For the investigation of size and morphology of the nanofibers, SEM (AIS2100 model, Seron Technology Co., South Korea) at 25 kV voltage was used. First, dried nanofibers were gold-coated with a sputter-coater (SC7620 model, Quorum Technologies co., UK) for 90 s. Image J software was used to measure the diameter of nanofibers.

Contact Angle Measurement

Contact angle measurement was done to investigate the hydrophilicity of the scaffolds. First, 5 μL of distilled water was placed on scaffolds, after 10 s, pictures from the interface between water droplet and scaffolds were taken by a Dino Camera. Image J software was used to measure the contact angle.

Isolation and Characterization of BMSCs

Animals were kept under stable state conditions and all procedures were accepted by the Ethics Committee of Shahid Beheshti University of Medical Sciences (IR.SBMU.RETECH.REC.1398.001) based on National Institutes of Health Principles of Laboratory Animal Care (NIH publication no. 85–23, revised1985).

Briefly, rat was sacrificed, and the femur as well as tibia was separated. The bone marrow was extracted with a syringe needle (G 18) containing DMEM medium containing 10% FBS plus 0.25% trypsin and 1 Mm EDTA. Bone marrow cells were cultured in 0.75 cm^2 flasks with DMEM/F12 medium containing 10% FBS, 100 $U.mL^{-1}$ penicillin, 100 $mg.mL^{-1}$ streptomycin, and glutamine. The flask was placed in an incubator at 37°C and 5% CO_2. After 24 h, floating cells were removed, and the medium was replaced daily. After reaching confluency, the cells were removed from flask by using 0.25% trypsin and 1 mM EDTA, after 5 mins at 37°C. Then, the cell suspension was cultured for four passages again. These cells were used to analyze scaffold biocompatibility and differentiation study. As mentioned, in order to differentiate BMSCs toward OLCs, they are transdifferentiated to NSFs, and then to NSCs. Finally, NSCs were seeded on the scaffolds to induce differentiation toward OLCs. For the characterization of BMSCs, the flowcytometry analysis was performed. Adherent cells were trypsinized and dissociated by Trypsin/EDTA and re-suspended in a completely fresh medium and then transferred to new flasks at a density of 1×10^4 $cells.cm^{-2}$. Afterward, PBS was used to wash the fixed cells twice and the cells were incubated at 4°C with antibodies specific for the following antigens: CD34, CD45, CD90, CD44, Nestin, NF68, GFAP for 30 mins. Phycoerythrin was conjugated with primary antibodies, and fluorescence-activated cell sorting (FACS) which is a specialized type of flow cytometry was carried out (Becton Dickinson, USA), and flow cytometry analysis was done by a Partec CyFlow Space cytometer system using FloMax software.

Analysis of Cell Viability on Scaffold

BMSCs were used to evaluate the effect of T3 and PAG on the biocompatibility of the scaffold using the MTT test. First, this test was performed for scaffolds with different percentages of PAG without the presence of chitosan NPs, and then for scaffolds containing chitosan NPs loaded with T3. Cells were seeded on the scaffolds in 96-well with 5000 $cells.cm^{-2}$ cell density. The viability of the seeded cells was evaluated after days 1, 3, 5 and 7 with three replications for each sample. After each time interval, cells were washed with sterile PBS followed by adding 100 µL fresh DMEM/F12 medium as well as 10 µL of 5 $mg.mL^{-1}$ MTT dye. The plates were incubated for 2–4 h at 37°C. After the formation of purple precipitate, the medium was removed and 100 µL DMSO was added to each well. After leaving the covered plate in a dark place for 2 h, the content of the plate was transferred to a new 96-well plate and the absorbance at 570 nm was measured using Biotek ELISA reader. In addition, to observe the morphology of cells on scaffolds, the cells were washed with PBS and then fixed with 2.5% glutaraldehyde solution for 2 hr. Dehydration process was done by immersing the samples in different concentrations of ethanol (50%, 70%, 90%, and 100% v/v) for 15 min. After dehydration, the samples were gold-coated and observed under SEM.

NSF Formation and NSC Differentiation

NSF formation was carried out according to a previous study.[11] Extracted BMSCs were cultured in DMEM/F12 supplemented by 2% B27, 20 $ng.mL^{-1}$ bFGF, 20 $ng.mL^{-1}$ EGF, 100 $U.mL^{-1}$ of penicillin, and 100 $mg.mL^{-1}$ of streptomycin for 4 days, after which the cells formed NSF structure. After 7 days of culturing NSFs, they were dissociated by 0.25% trypsin and 1 mM EDTA and cultured on petri dish coated by poly-lysine in DMEM/F12 medium containing 5% FBS, 10 $ng.mL^{-1}$ EGF, 10 $ng.mL^{-1}$ bFGF, 1% B27, 100 $U.mL^{-1}$ penicillin, and 100 $mg.mL^{-1}$ streptomycin for 7 days in order to induce differentiation toward NSCs.[11]

Differentiation Analysis of BMSCs to NSCs

To evaluate the differentiation of BMSCs to NSCs flowcytometry analysis was performed as described before. Nestin, NF160, and NF68 markers as neural stem cell markers and GFAP as astrocyte marker were selected for flowcytometric analysis.

OLCs-Like Cell Differentiation

In order to differentiate NSCs to OLCs, first NSCs were seeded on the scaffolds with a cell density of 25,000 $cells.cm^{-2}$ and treated with basal medium supplemented with 10 $ng.mL^{-1}$ bFGF, 5 $ng.mL^{-1}$ PDGF-AA, and 200 ng.

mL^{-1} heregulin. The cells were cultured on five scaffolds groups for 14 days.

Differentiation Analysis of NSCs to OLCs

After 14 days of cell culture on the scaffolds, the differentiation of NSCs to OLCs was evaluated using different techniques. After detaching the cells from the scaffold by using Trypsin/EDTA, RT-PCR and immunostaining were used to analyze the expression of oligodendrocyte markers including O1, O4, and MOG. Furthermore, flow cytometry analysis was carried out for PDGFR-α, Olig 2, MBP, and GFAP markers as described before.

mRNA Expression

After 14 days, the gene expression of O4, O1, and MOG and glyceraldehyde 3-phosphate dehydrogenase (GAPDH) were assessed by performing Reverse Transcriptase PCR (RT-PCR) assay. The RNX-Plus Kit was used with 2 µg of total RNA from each sample and then DNase I was added to them. Optical density measurements and electrophoresis on 1% agarose gel were adopted in order to assess both the purity and integrity of the extracted RNA. The first-strand cDNA Synthesis Kit was used for the purpose of converting extracted RNA (1 µg) to cDNA. To amplify cDNA, 35 PCR cycles were run including denaturation at 95°C for about 45 s, annealing at 60°C for about 45 s, and elongation at 72°C for 30 s using 50 ng of cDNA. Finally, 2% agarose gel was used to separate the products and ethidium bromide was added to visualize the products under UV light. All the experiments were performed in triplicate and repeated at least 3 times. Both forward and reverse primer sequences, the final size of the product and PCR conditions are tabulated in Table 2.

Immunocytochemistry

In order to fix the cultured cells, 4% paraformaldehyde in 0.1 M phosphate buffer (pH 7.4) was used for 20 min. After the process of permeabilization, 5% bovine serum albumin was used for 30 min to block the cells. Immunostaining method was performed on BMSCs and OLCS cells. The mouse anti-O4 monoclonal antibody (1:100), mouse anti-O1 monoclonal antibody (1:100) and mouse anti-MOG monoclonal antibody (1:1000) as a specific marker for mature oligodendrocytes were used. FITC conjugated rabbit anti-mouse secondary antibody (1:100) was added to cells for the duration of 2 h at 25°C. The cells were counterstained using 1:10,000 ethidium bromide for 1 min.

Static Analysis

The one-way analysis of variance (ANOVA) was performed for statistical analysis using Tukey's post hoc test. The data were expressed as mean ± SEM and P-value was considered to be statistically significant when the value was less than 0.05 ($p<0.05$).

Results and Discussion

The Analysis of Conductive Nanofiber Scaffold

Morphological Characterization

SEM images were taken in order to assess gelatin nanofibers with and without PAG and PCL nanofibers morphology as shown in Figure 2A. As shown in Figure 2B, the diameter of the gelatin nanofibers containing PAG has been changed as a function of PAG percentage. By increasing the percentage of conductive nanoparticles from 1% to 2%, the diameter of the fibers was reduced from 360 to 263 nm due to the higher conductivity of the polymer solution.[23] It should be noted that a low percentage of PAG including 1% and 2% did not affect the polymer solution viscosity significantly. However, by increasing the concentration of PAG from 2% to 3%, the fiber diameter increased to 372 nm which is caused

Table 2 Primer Sequence for RT-PCR Analysis

Gene	Primer Sequence	Gene Size (Base Pair)
GAPDH	Forward: 5′-ACCCAGAAGACTGTGGATGG-3′ Reverse: 5′-CACATTGGGGGTAGGAACAC-3′	200
O1	Forward: 5-GGCCGCGCTCGTGCACCTGG-3 Reverse: 3-GGGCTGCCTGC ACCCAGCGCC-5	210
O4	Forward: 5-GCTAACCAGCCGTCCGAGCCG-3 Reverse: 3-TTCATCAAGGTTCACAACGAG-5	185
MOG	Forward: 5′- AGGAAGGGACATGCAGCCGGAG −3′ Reverse: 5′- CTGCATAGCTGCATGACAACTG −3′	180

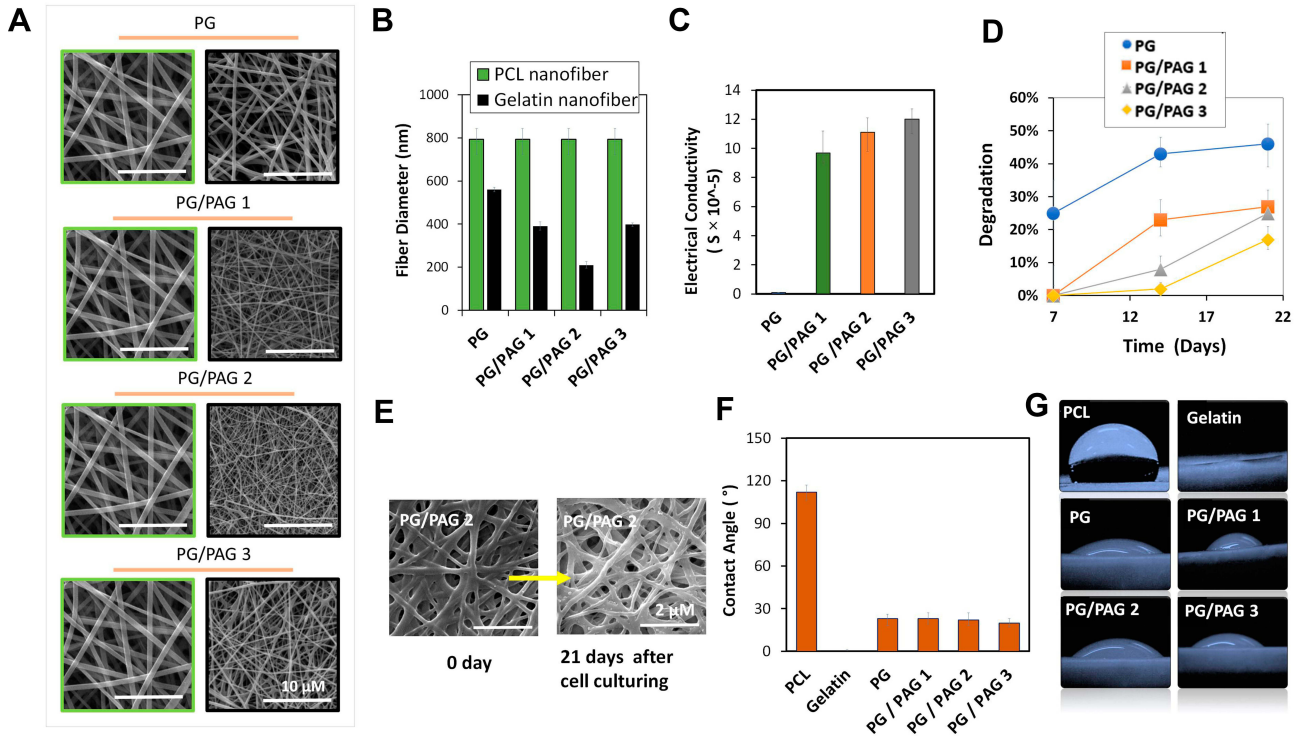

Figure 2 Fabrication and analysis of conductive PAG-loaded gelatin nanofiber scaffold. (**A**) SEM graphs of PCL/gelatin nanofibers, left images show PCL nanofibers and the right images show gelatin nanofibers (**B**) nanofiber diameter, (**C**) degradation rate, and (**D**) SEM images of PG/PAG 2 at day 0 and day 14 after cell culturing, (**E**) electrical conductivity of the scaffolds, (**F**) contact angle measurement of scaffolds, (**G**) the condition of water droplet on different scaffolds.

by the fact that a high percentage of PAG increased the gelatin solution viscosity. Indeed, in case of using 3% of PAG, the effect of higher viscosity of gelatin solution outweigh its higher conductivity which led a bigger diameter of gelatin nanofibers.

Electrical Conductivity Measurement

Free electron in polymer backbone conducts electrical current. Since the purpose of this study was to synthesize scaffold to mimic the natural microenvironment of NSCs in order to induce differentiation toward OLCs, the electrical conductivity of scaffold was considered as an important parameter. The use of conductive polymers would mimic OLCs natural microenvironment. Ghasemi-Mobarakeh et al reported that applying direct current to polyaniline/gelatin (15:85) with electrical conductivity of 0.02×10^{-6} S amended the NSCs proliferation and neurite outgrowth;[24] likewise, Li et al used polyaniline/PCL nanofibers with electrical stimulation to culture human umbilical vein endothelial cells (HUVECs) and reported promotion in growth for the cultured cells in the presence of conductive polymer.[25] As shown in Figure 2C, the electrical conductivity of nanofiber scaffolds was PAG dose-dependent. In comparison to the results reported by Baniasadi et al, the conductivity of the fabricated nanofiber scaffolds in the present study declined due to the presence of PCL nanofibers although its conductivity is around 1.2×10^{-5} S/cm which is still in an appropriate range to be used for neural tissue engineering.[15] Lee's group seeded PC12 cells on nanofiber scaffolds coated with polypyrrole and applied the potential of 10 and 100 mV/cm to them. Their experiments demonstrated that electrical stimulation promoted neurite outgrowth compared to the non-stimulated situation. This group also showed that the potential of 10mV/cm causes higher neurite outgrowth in comparison with the potential of 100 mV/cm.[26]

Biodegradability of Scaffold

Scaffold degradation time is a decisive parameter in the design of the scaffold. The low degradation rate of conductive polymers is one of their disadvantages.[27] Therefore, the combination of conductive polymers with degradable polymers can improve the biodegradability of the final scaffold. The ability of the gelatin to dissolve in water and its hydrolysis, as well as enzymatic degradation, has made it useful for the construction of different scaffolds.[28,29] Various strategies have been proposed to

increase gelatin resistance in physiological environments, including the use of crosslinking agents or their combination with synthetic polymers.[30] In this regard, the use of PCL as synthetic polymer and addition of PAG nanoparticle to gelatin solution were proposed to optimize the scaffold degradation rate. Since the degradation rate of PCL and polyaniline is very low, and the rate of degradation of gelatin is too fast, their combination may optimize the rate of degradation. The results of the biodegradation test carried out for 21 days confirmed the effect of PAG on the reduction of scaffold degradation rate (Figure 2D). Baniassadi et al showed that the rate of degradation was reduced by increasing the concentration of PAG in gelatin-chitosan scaffolds.[15] Soleimani et al also observed that the duration of degradation was increased by adding PAG to the gelatin scaffold.[31] As shown in Figure 2D, by increasing the percentage of PAG in the hybrid scaffold, the degradability of samples has been decreased. However, the scaffold degradation rate in the absence of PAG was relatively fast. In addition, the SEM image of PG/PAG 2 scaffold used to study cell analysis showed no significant morphological changes in nanofibers after 21 days of cell culturing (Figure 2E).

The Hydrophilicity of Scaffold

The hydrophilicity of scaffold is one of the most important parameters in cell attachment. However, PCL nanofibers had a hydrophobic surface.[32] In this study to improve the hydrophilicity of PCL nanofibers, gelatin nanofibers were employed. PCL nanofibers showed a contact angle of 112°, which is in the range of hydrophobic materials. As shown in Figure 2F and G, dual-electrospinning of gelatin with PCL solution decreased the contact angle of scaffold from 112° to 23°. Since the polyaniline used to synthesize PAG was in salt form[16] and its contact angle was within the range of hydrophilic materials,[24,33] it was expected that its addition to gelatin could decrease the contact angle. However, the addition of this substance could not change the scaffold contact angle significantly due to low concentration of applied PAG in the system, which was in accordance with the results reported by Ghasemi Mobarakee et al.[24] Jun et al[34] showed only 3° reduction in the contact angle of their scaffold in the presence of 30% polyaniline.

BMSCs Characterization

Flow cytometry was performed to confirm the existence of BMSCs as shown in Figure 3A. In this analysis, CD44, CD90, and CD 106 markers as mesenchymal stem cell markers and CD45 as hematopoietic stem cells marker were used. Flowcytometric analysis showed that cultured cells were positive for mesenchymal markers CD29 (94.5%) (D), CD73 (99.4%), CD105 (99.9) and negative for hematopoietic cell markers CD45 (3.67%).

Evaluation of BMSCs Proliferation on Conductive Nanofiber Scaffold

MTT assay was performed to find the optimum percentage of PAG and T3-loaded chitosan NPs. Considering PAG structure, graphene plates are mounted on the center of NPs and polyaniline chains sited on top of graphene plates;[35] hence, the effect of polyaniline and graphene may conduct cell behaviors. As shown in Figure 3B, scaffolds containing 2% of PAG showed the highest cell proliferation. As shown in Figure 3C, cells exhibited more flattened morphology on PG/PAG 2 compared to PG scaffold. The results of this test revealed a high dependency of cellular behaviors on the percentage of PAG in the scaffolds. Kim and colleagues reported that chitosan-containing graphene substrates improved cell adhesion of human mesenchymal cells while cell proliferation decreased by adding a higher amount of graphene to chitosan because it causes higher differentiation rather than proliferation. This group claimed that nanotopographical cues of graphene incorporated in chitosan improved cell spreading thereby enhancing interactions between cells and cell-substrate. They have reported that the presence of graphene on the surface of the chitosan substrate and the formation of surface nano topography has improved the interaction of the cells with the surface.[36] In addition, polyaniline can increase reactive oxygen species (ROS) content in cells and cause cell death.[37] Besides the effect of PAG on cell behavior, nanofiber size can potentially influence cell viability and spreading. According to the result in this study, the scaffold with smaller nanofiber size showed the highest biocompatibility. Noreiga et al reported the effect of nanofiber size on cell viability. They reported similar results and showed that cell viability on the scaffold with smaller nanofiber diameter was higher than the other scaffolds.[38] According to the results of MTT assay and SEM images, the biocompatibility of PAG was completely dependent on its content in the scaffold. The lowest amount of cell proliferation was observed for PG/PAG3 due to the high concentration of polyaniline and its cytotoxicity.[37] Scaffolds

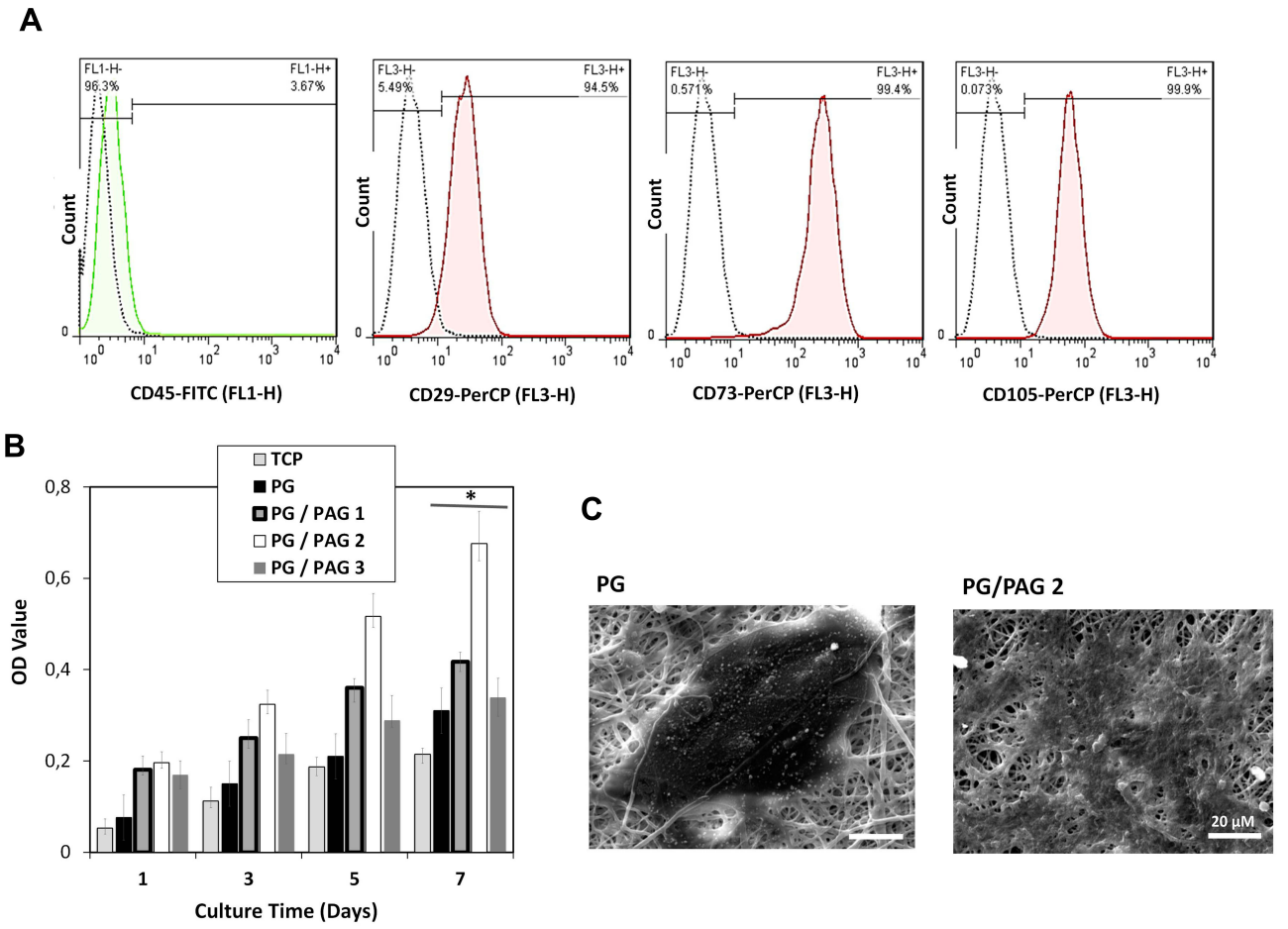

Figure 3 Characterization of BMSCs and cell viability analysis of BMSCs on scaffold. (**A**) The flow cytometry analysis of CD44, CD90, CD 106 and CD45 for BMSCs, (**B**) cell viability on PCL/gelatin scaffolds containing various amount of PAG, *Indicates significant difference of $p < 0.05$, (**C**) cell spreading on two different scaffold.

incorporating 2% PAG were considered as the optimum scaffold and was used for further experiments.

The Analysis of T3-Loaded Conductive Nanofiber Scaffold

The effect of NPs on PCL/gelatin scaffold was investigated by analyzing PCL nanofiber morphology, release study of T3, cell viability, and differentiation. As shown in Table 3, there were five different groups analyzed in this step denoted as PG, PG/PAG 2, PG/PAG 2/1% NPs, PG/PAG 2/2% NPs and PG/PAG 2/3% NPs.

Chitosan NPs Characterization

One of the methods to fabricate chitosan NPs is based on ionic gelation methods. In this method, positive-charged amine groups in chitosan will interact with negatively

Table 3 Experimental Groups for Scaffold Fabrication with Varied T3-Loaded Chitosan NPs Content

Sample	Condition
PG	Cells were cultured on PCL/gelatin scaffold without PAG and without chitosan NPs.
PG/PAG 2	Cells were cultured on PCL/gelatin scaffold containing 2% PAG and without chitosan NPs.
PG/PAG 2/1% NPs	Cells were cultured on PCL/gelatin scaffold containing 2% PAG and 1% T3-loaded chitosan NPs.
PG/PAG 2/2% NPs	Cells were cultured on PCL/gelatin scaffold containing 2% PAG and 2% T3-loaded chitosan NPs.
PG/PAG 2/3% NPs	Cells were cultured on PCL/gelatin scaffold containing 2% PAG and 3% T3-loaded chitosan NPs.

Notes: All above samples were cultured in DMEM/F12 base medium containing 10 $ng.mL^{-1}$ bFGF, 5 $ng.mL^{-1}$ PDGF-AA and 200 $ng.mL^{-1}$ heregulin.

charged tripolyphosphate molecules.[39] T3 is a type of hormone derived from the amino acid tyrosine. In order to increase the loading of nanoparticles, the interaction between the positive and negative groups between chitosan and T3 was required. The isoelectric point (PI) of chitosan is approximately 6.2, and pK of hydroxyl phenol group of T3 is 8.5.[40] Adjusting the pH of the chitosan solution below the PI of chitosan resulted in a positive charge of chitosan chains.[21] While the pH of TPP solution is around 9, adding T3 solution to TPP solution enhanced the ionization of the hydroxyl group of T3 which caused a higher negative charge. After optimizing the operating conditions such as chitosan and TPP concentration, stirring speed, volume ratio of chitosan solution to TPP solution, and T3 concentration, T3-loaded chitosan NPs were synthesized. The procedure is shown schematically in Figure 4A. LC and EE % of T3 in chitosan NPs reported to be 3.8% and 87%, respectively. The size distribution of T3-free chitosan NPs in terms of the number obtained by the DLS is shown in Figure 4B. Besides, by loading T3 in the chitosan NPs, the average diameter of synthesized chitosan NPs was increased from 78 nm to 91 nm. In addition, the FE-SEM micrograph images showed chitosan nanoparticles with roughly spherical morphology and less diameter size compared to DLS result due to the dehydration of nanoparticles (Figure 4C).

Morphological Characterization of T3-Loaded Nanofiber Scaffold

SEM images of five different groups of PCL/gelatin nanofibers with and without T3-loaded chitosan nanoparticles are shown in Figure 5A. As shown in Figure 5B, the diameter of the PCL nanofibers without chitosan NPs was 793 ± 20 nm. After adding 1% of chitosan NPs to the PCL solution, the diameter of nanofiber increased to 821 ± 20 nm due to the higher viscosity of polymer solutions. On the other hand, by increasing the percentage of chitosan NPs to about 2%, the conductivity of PCL solution increased, and consequently, the diameter of PCL nanofibers was reduced to 750 ± 72 nm due to higher amount of tween 80 in PCL solution.[17] Again, increasing the percentage of chitosan NPs up to 3% increased the viscosity of the PCL solution which overcame the higher conductivity and led to increased PCL nanofibers diameter to 780 ± 6 nm. However, the overall effect of chitosan nanoparticles on the size of PCL nanofibers was not significantly noticeable.

Release Profile of T3 from Conductive Bioactive Nanofibers

According to Table 3, hybrid PCL/gelatin scaffolds containing 1, 2 and 3 (%) T3-loaded chitosan NPs denoted as PG/PAG 2/1% NPs, PG/PAG 2/2% NPs, and PG/PAG 2/3% NPs, respectively, were used to obtain the

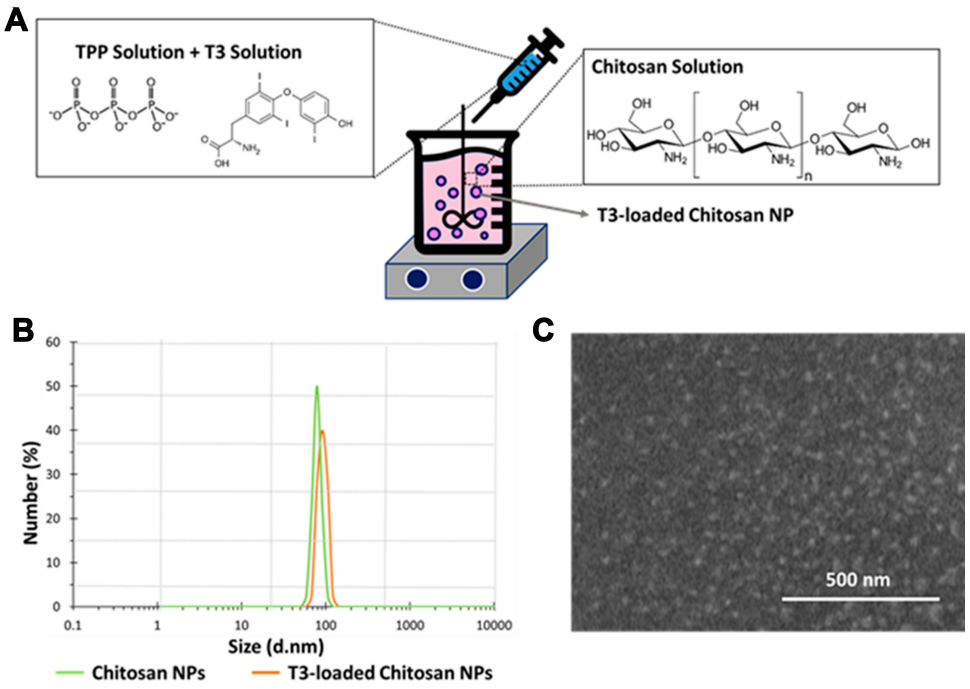

Figure 4 (**A**) Schematic procedure for chitosan NPs synthesis, (**B**) chitosan NPs size and distribution, (**C**) FESEM image of dried chitosan NPs.

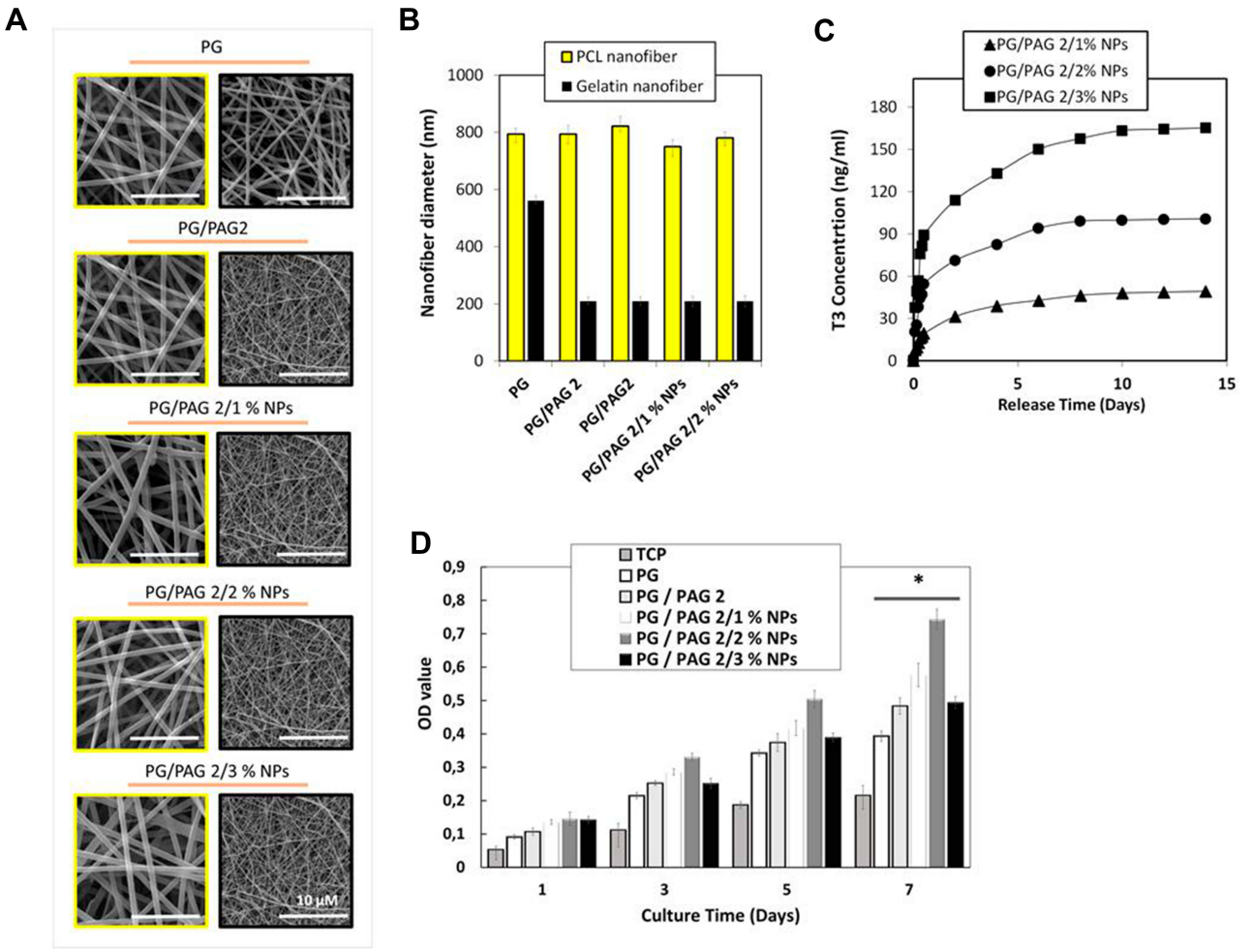

Figure 5 Characterization of T3-loaded nanofiber scaffold. (**A**) SEM graphs of PCL/gelatin nanofibers, left images show PCL nanofibers containing T3-loaded chitosan NPs and the right images show gelatin nanofibers containing PAG nanoparticles, (**B**) nanofiber diameter, (**C**) release profile of T3 from PCL/gelatin scaffolds containing various amount of T3-loaded chitosan NPs, (**D**) BMSCs viability on PG, PG/PAG 2, PG/PAG 2/1% NP, PG/PAG 2/2% NP, and PG/PAG 2/3% NP %; *Indicates significant difference of $p < 0.05$.

optimum concentration of chitosan NPs in the scaffold to induce differentiation of NSCs to OLCs. According to a previous study reported by Abbaszadeh et al concerning the differentiation of NSCs to OLCs using T3, the optimal concentration of this differentiating factor in the culture medium was reported to be 25 $ng.mL^{-1}$.[11] Based on this optimal concentration, the amount of chitosan NPs containing T3 in the scaffold was selected. Three different scaffolds containing various amount of chitosan NPs were electrospun. The amount of T3 released from the scaffolds during 14 days had three different levels including fast, medium, and slow rates. As shown in Figure 5C, the concentration of T3 released from PG/PAG 2/1% NPs, PG/PAG 2/2% NPs, and PG/PAG 2/3% NPs scaffolds over a period of 4 days reached to 39, 82, and 133 $ng.mL^{-1}$, respectively.

The Analysis of Cell Viability of Cells Cultured on Conductive T3-Loaded Nanofibers

After finding the optimal concentration of PAG, the optimal percentage of chitosan NPs containing T3 was investigated by culturing BMSCs on PG/PAG 2 scaffolds having various percentages of T3-loaded chitosan NPs and MTT assay was performed. The observed results of MTT assay for the first and third days showed no significant change among different groups, while MTT results for the fifth and seventh days. showed a significant increase in cell attachment on PG/PAG 2/2% NPs as shown in Figure 5D. Abbaszadeh and colleagues used T3 as a differentiating factor for differentiation of neural precursor stem cells to OLCs and found the effective range of concentration of T3. Hence, out of the reported range, T3 would not be effective, or it may cause cytotoxicity. This research group reported that the highest viability was observed

at a concentration of 25 ng.mL^{-1}, and at the concentrations of 50, 100 and 200 (ng.mL^{-1}) it caused cytotoxicity.[11] Based on the obtained results, scaffold containing 2% and 3% of T3-loaded chitosan NPs were considered to be the most and the least biocompatible samples among the other groups, respectively.

Evaluation of the Differentiation of BMSCs Toward NSCs

The differentiation of NSCs was analyzed with NF68, NF160, NESTIN, and GFAP markers. NF68, Nestin, NF160, and GFAP were analyzed by flow cytometry. The three markers NF68, NF160 and Nestin were both specific markers for NSCs although the GFAP marker was considered as a specific marker for astrocyte. As shown in Figure 6A, the flowcytometric analysis showed that cultured cells were positive for neural stem cell markers Nestin (91.1%), NF160 (98.9%), NF68 (91.9), and negative for astrocyte marker GFAP (2.85%).

Evaluation of the Differentiation of NSCs Cultured on Conductive Bioactive Scaffold Towards OLCs

RT-PCR

As previously mentioned, RT-PCR analysis was used to evaluate the differentiation of OLCs. The qualitative and quantitative results of RT-PCR analysis are shown in Figure 6B and C, respectively. As can be seen, scaffolds containing different concentrations of T3 have different effects on cell differentiation. mRNA levels of O4: a transcription factor in pre-OLCs, O1: a transcription factor in immature OLCs, and MOG: a transcription factor in mature OLCs were observed by RT-PCR analysis.[41–43] Among all the scaffolds, the ones containing 1% of T3-loaded chitosan NPs (PG/PAG2/1% NP) showed less effect on cell differentiation, and the cells exhibited less expression of O4, O1, and MOG genes due to its low concentration of T_3 compared with the cells cultured on the scaffold containing 2% T3-loaded chitosan NPs (PG/

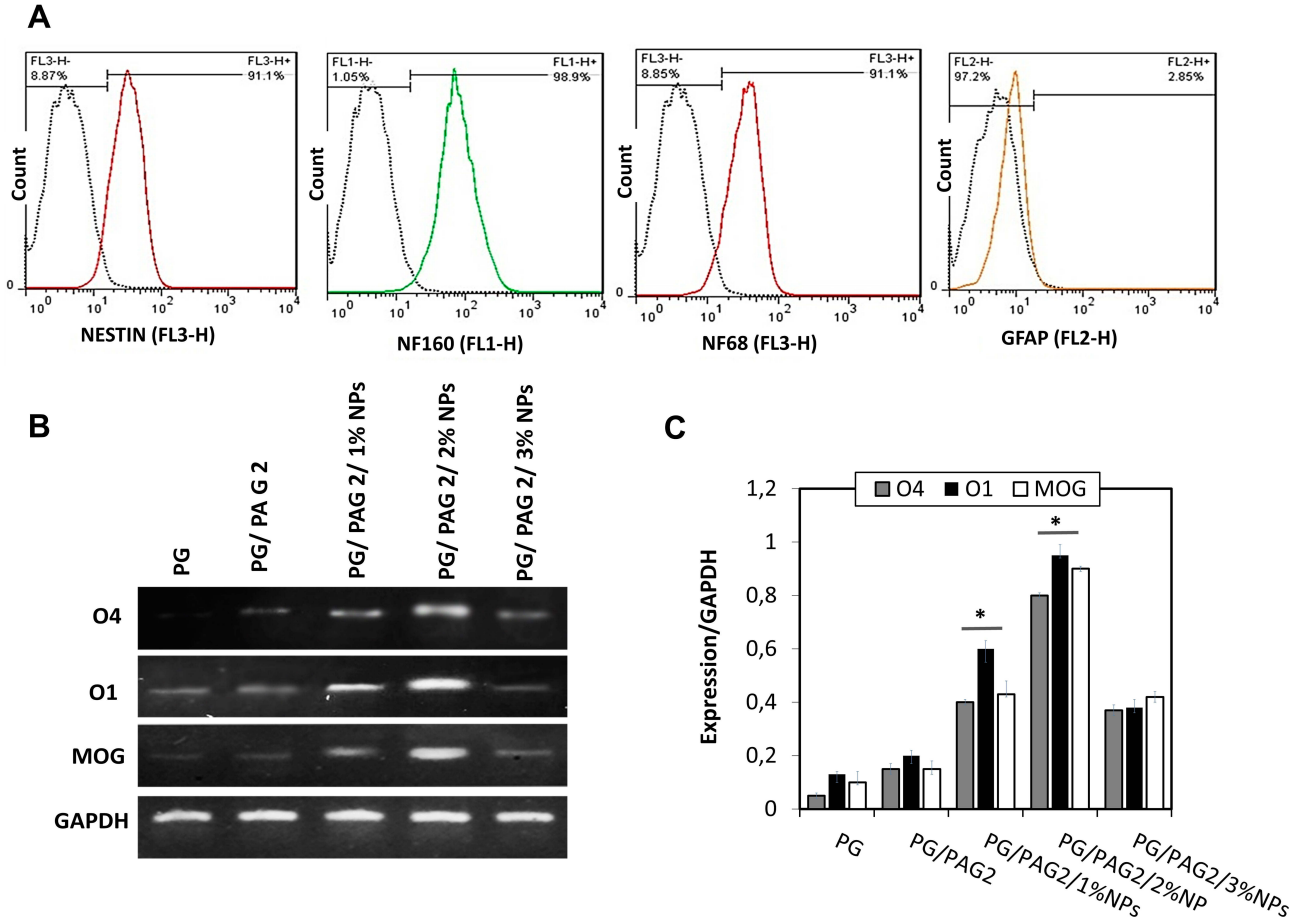

Figure 6 Characterization of NSCs and the differentiation of NSCs to OLCs on scaffolds. (**A**) Flow cytometry analysis of NF68, NF160, Nestin, and GFAP, (**B**) RT-PCR analysis for O1, O4, and MOG genes, (**C**) RT-PCR quantitative data for O1, O4, and MOG. Note, *Indicates a significant difference of $p < 0.05$.

PAG2/1% NP) which showed relatively higher expression of O4, O1, and MOG. The cytotoxicity caused by the high concentration of T3 embedded in the scaffold containing 3% T3-loaded chitosan NPs (PG/PAG2/3% NP) caused cell death as shown by MTT assay results. Generally, T3 plays a very important role in the growth and maturity of OLCs. Some myelin genes are directly controlled by thyroid hormone receptors. Therefore, the presence of T3 is essential for the differentiation and maturity of OLCs at the later stages of differentiation.[11] As mentioned before, pre-OLCs and immature OLCs express O4 and O1, respectively. The expression of these genes in large amounts will be a stimulus to differentiate NSC to mature OLCS. MOG gene is expressed by mature OLCs. This gene is considered as one of the most important functional genes for OLCs. T3 plays an important role in the functional maturity of immature OLCs and increasing the expression of MOG.[11,41,43]

Immunostaining

Three important cell surface markers including O4, O1, and MOG were used to evaluate the differentiation of NSCs to pre-OLCs, immature OLCs, and mature OLCs, respectively. The evaluation of expression of these markers for cells seeded on scaffolds without T3 showed that NSCs did not differentiate significantly from OLCs. However, the presence of these markers was significantly increased for the cells cultured on scaffolds containing T3. The qualitative and quantitative results of immunocytochemistry analysis are shown in Figure 7A and B, respectively. The use of nanofibers to simulate the axonal environment to direct the differentiation of NSC is a method used by different groups.[8,44] Lee and colleagues used polystyrene with various fiber diameters to study the differentiation and myelination of precursor OLCs. This research team showed that the process of differentiation and myelination of these cells took place without the need for the presence of neurons and their simultaneous co-culturing. Thus, providing a microenvironment similar to axon can be very effective for the differentiation and maturity of OLCS. As can be deduced from the results of immunostaining, the expression level of these three markers were different for the scaffolds with varied T3-loaded NPs content. As shown in Figure 5E and F, a small population of cells cultured on PG and PG/PAG 2 expressed these three markers, which may be attributed to the effects of fiber morphology and also other supplementaries including bFGF, PDGF, and heregulin used in culture medium to promote the differentiation at the early stage.[11] Higher number of cells cultured on PG/PAG 2/1% NPs expressed O4 compared to O1 and MOG. In other words, a lower concentration of T3 in the medium caused a higher population of pre-OLCs or immature OLCs than mature OLCs. Eighty-five percent of the cells cultured on PG/PAG 2/2% NPs expressed O1 marker and 80% of the cells cultured on the same scaffold expressed MOG

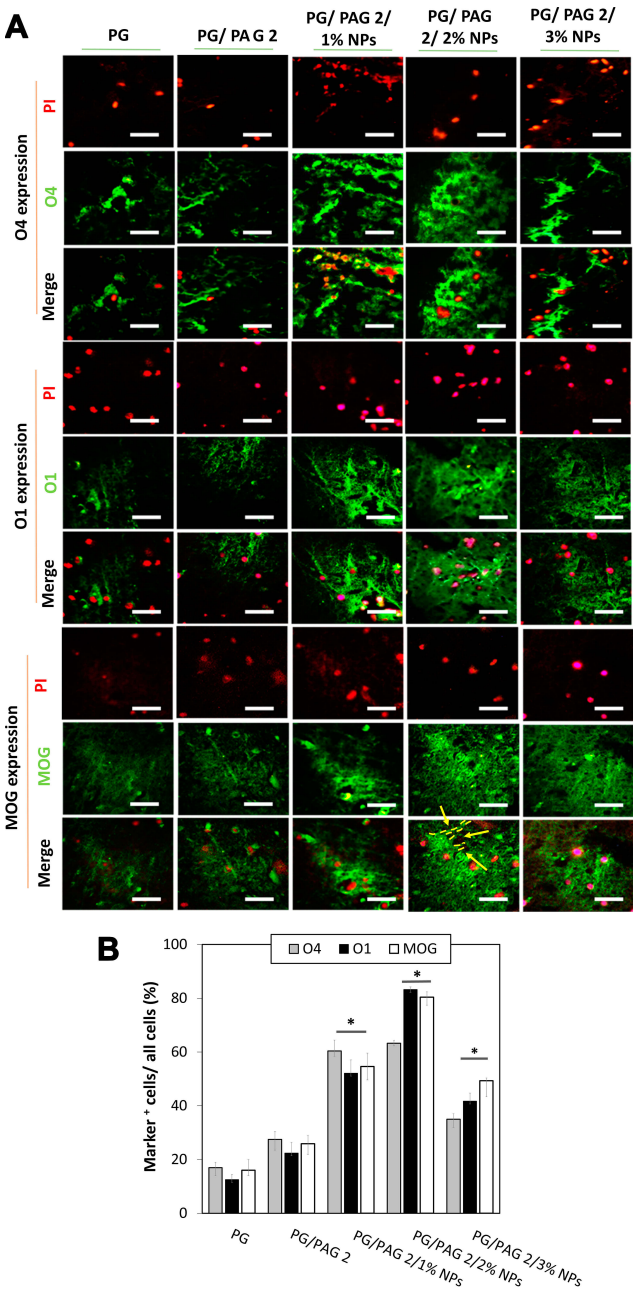

Figure 7 The differentiation of NSCs to OLCs on scaffold. (**A**) qualitative and (**B**) quantitative immunocytochemistry analysis of the transdifferentiated BMSCs into OLCs, *Indicates a significant difference of $p < 0.05$, scale bar = 20 μM. Yellow arrows in (**A**) show cell process extension.

marker. MOG was considered as a marker for adult OLCs, and its high percentage indicated the efficiency of the differentiation and secretion of glycoprotein associated with myelin plates.[11] It was deduced that the concentration and the release rate of T3 were sufficient to differentiate pre-OLC to immature and mature OLCs. In the case of cells cultured on PG/PAG 2/3% NPs, MOG expression was higher in comparison to O1 and O4. Although the concentration of T3 was high enough to promote the differentiation of NSCs to mature OLCs, but more population of the cells were died and did not show significant expression of markers due to the high concentration of T3, which may cause toxicity. In conclusion, in this study, a controlled release of T3 caused differentiation of NSFs into OLCs which mimics the fetal growth when T3 is produced to stimulate differentiation in CNS.[45]

Flow Cytometry Analysis

For further evaluation of oligodendrocyte differentiation on PG/PAG 2/2% NPs scaffold, flow cytometry analysis was carried out. In fact, the oligodendrogenesis may go through several differentiation stages for the differentiation of NSC into OLCs, including precursor, immature, mature and functional OLC that produces myelin and these stages are characterized by distinct morphological and antigenic changes and specific markers are expressed during this differentiation process including PDGFR-α, O4, OLIG2, O1, GFAP, MBP, and MOG.[11] PDGFR-α, Olig 2 as early markers and MBP as mature OLC were selected. As shown in Figure 8A, cultured cells were positive for immature OLC markers, PDGFR-α (85.3%), Olig 2 (87.16%), and mature marker, MBP (80.2%). These data exhibited that NSCs cultured on PG/PAG 2/2% NPs scaffold showed a high level of expression of reliable oligodendrocyte markers. One of the important mitogens for oligodendrocyte progenitor cells is PDGF, which induces the differentiation and proliferation of NSC into OLC. PDGF induces a specific number of cell divisions. PDGF can block the intracellular signaling pathways starts from the PDGF receptor to the expression of the PDGFR-α gene, and thereby it could affect oligodendrocyte progenitor cell development and proliferation.[11] Olig2 transcription factors are expressed by both oligodendrocyte precursor cells and mature oligodendrocyte. It was reported that its expression is important for neural progenitor cell differentiation into the oligodendroglial lineage but its overexpression may induce the NSCs differentiation into mature oligodendrocytes based on an in vitro study.[41] By knocking down the Olig2 gene in the immature oligodendrocytes, the degree of maturation was increased, which was correlated with

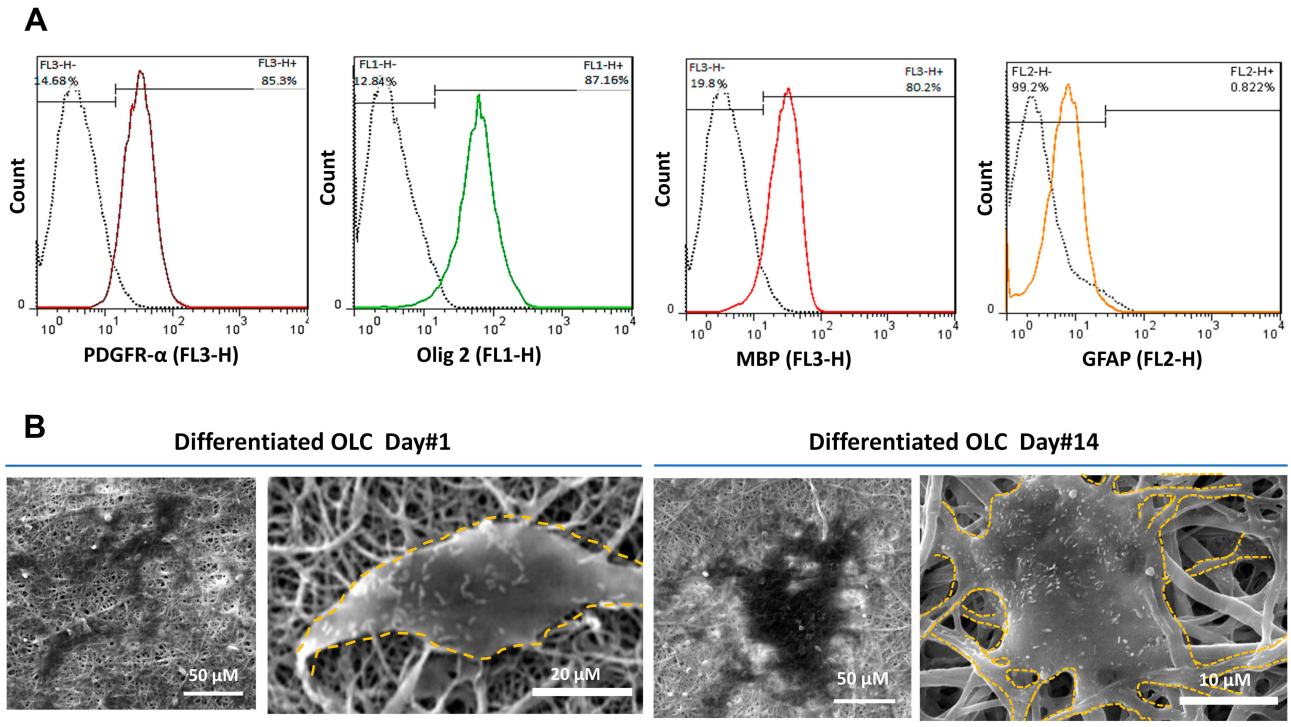

Figure 8 Characterization of the differentiation of NSCs to OLCs on PG/PAG 2/2% NP scaffold. (**A**) Flow cytometry analysis of the expression of PDGFR-α, Olig 2, MBP, and GFAP markers in differentiated OLCs, (**B**) SEM images of morphological changes of differentiated OLC cultured on PG/PAG 2/2% NP scaffold at day 1 and day 14.

myelination.[11,41] To show the selective differentiation of NSCs towards OLCs, the expression of GFAP as an astrocyte marker was analyzed. The percentage of positive cells for GFAP marker indicated the selective differentiation of NSCs to OLCs. In addition, the presence of MBP as an indicative marker of myelinating OLC[46] for NSCs cultured on PG/PAG 2/2% NPs scaffold showed that the concentration of T3 and the morphology of nanofiber microenvironment strongly affected not only the differentiation of NSCs to OLC but also the maturation of the cells to myelinating OLC stage. Both MBP and MOG are key markers for both maturity and functionality and they are expressed by the differentiated oligodendrocytes. Thyroid hormone receptors could regulate MBP and MOG genes because they have thyroid hormone response elements as an enhancer-like element.[41]

Morphological Analysis of NSC and OLC

As shown in the results, the highest amount of expression of all marker genes was observed for the cells cultured on PG/PAG 2/2% NP compared to the other groups. In addition to T3 effect on guiding oligodendrocyte differentiation,[11] it should be noticed that probably the morphology of nanofibers also had an effect on directing oligodendrocyte differentiation. Christopherson et al reported that NSCs cultured on 283-nm fibers showed a significant increase in oligodendrocyte differentiation due to the multi-direction guidance of nanofibers and cell spreading compared to the cells cultured on nanofibers with bigger diameter.[47] As shown in Figure 8B, differentiated NCSs on PG/PAG 2/2% NP scaffold spread in different directions and showed extended cell morphology similar to oligodendrocytes. The fiber size of gelatin nanofiber in PG/PAG 2/2% NP scaffold is in the range that is favorable for oligodendrocytes due to its morphological resemblance to axons.[8] As shown in Figure 8B, the differentiation of NSCs to OLCs caused the morphological changes. After 14 days of differentiation process of spindle-like NSCs on PG/PAG 2/2% NP scaffold, cells show the extension of their process, which is one of the most characteristics of oligodendrocytes compared to NSCs. As shown in Figure 8B, since the size of cell processes is quite the same as the size of nanofibers, it is hard to distinguish the cell process from nanofibers.

Conclusion

Hybrid conductive nanofiber scaffolds of PCL and gelatin were fabricated using the co-electrospinning technique to direct stem cell fate. Using a nanofiber construct with sustained release of an induction factor, T3, with the potential for NSCs toward OLCs differentiation was demonstrated. In conclusion, the hybrid scaffold fabricated in this study providing an appropriate conductivity, surface topography and controlled release is a suitable substrate for the differentiation of NSCs to OLCs. This study strongly proves the potential use of bioactive PCL/gelatin nanofiber in the field of CNS tissue engineering and in vitro CNS disease model to study patients' own oligodendrocytes by isolating BMSCs.

Acknowledgments

This work was financially supported by the Iranian Stem Cell Council (Grant no. 11/93232). In addition, the authors acknowledge funding from Sina Trauma and Surgery Research Center (Tehran University of Medical Science and Health Services) and Hearing Disorders Research Center, Loghman Hakim Hospital, Shahid Beheshti University of Medical Sciences, Tehran, Iran.

Disclosure

The authors report no conflicts of interest in this work.

References

1. Leipzig ND, Wylie RG, Kim H, Shoichet MS. Differentiation of neural stem cells in three-dimensional growth factor-immobilized chitosan hydrogel scaffolds. *Biomaterials*. 2011;32(1):57–64. doi:10.1016/j.biomaterials.2010.09.031
2. Courtine G, Sofroniew MV. Spinal cord repair: advances in biology and technology. *Nat Med*. 2019;25:898–908.
3. Geissler SA, Sabin AL, Besser RR, et al. Biomimetic hydrogels direct spinal progenitor cell differentiation and promote functional recovery after spinal cord injury. *J Neural Eng*. 2018;15(2):025004. doi:10.1088/1741-2552/aaa55c
4. Kubinová Š. New trends in spinal cord tissue engineering. *Future Neurol*. 2015;10(2):129–145. doi:10.2217/fnl.14.71
5. Sher F, Rößler R, Brouwer N, Balasubramaniyan V, Boddeke E, Copray S. Differentiation of neural stem cells into oligodendrocytes: involvement of the polycomb group protein Ezh2. *Stem Cells*. 2008;26(11):2875–2883. doi:10.1634/stemcells.2008-0121
6. Rivet CJ, Zhou K, Gilbert RJ, Finkelstein DI, Forsythe JS. Cell infiltration into a 3D electrospun fiber and hydrogel hybrid scaffold implanted in the brain. *Biomatter*. 2015;5(1):e1005527. doi:10.1080/21592535.2015.1005527
7. Mekhail M, Almazan G, Tabrizian M. Oligodendrocyte-protection and remyelination post-spinal cord injuries: a review. *Prog Neurobiol*. 2012;96(3):322–339. doi:10.1016/j.pneurobio.2012.01.008
8. Shah S, Yin PT, Uehara TM, Chueng STD, Yang L, Lee KB. Guiding stem cell differentiation into oligodendrocytes using graphene-nanofiber hybrid scaffolds. *Adv Mater*. 2014;26(22):3673–3680. doi:10.1002/adma.201400523
9. Castelo-Branco G, Lilja T, Wallenborg K, et al. Neural stem cell differentiation is dictated by distinct actions of nuclear receptor corepressors and histone deacetylases. *Stem Cell Rep*. 2014;3(3):502–515. doi:10.1016/j.stemcr.2014.07.008

10. Noda M. Possible role of glial cells in the relationship between thyroid dysfunction and mental disorders. *Front Cell Neurosci*. 2015;9:194. doi:10.3389/fncel.2015.00194
11. Abbaszadeh H-A, Tiraihi T, Delshad A, et al. Differentiation of neurosphere-derived rat neural stem cells into oligodendrocyte-like cells by repressing PDGF-α and Olig2 with triiodothyronine. *Tissue Cell*. 2014;46(6):462–469. doi:10.1016/j.tice.2014.08.003
12. Nandoe Tewarie RS, Hurtado A, Bartels RH, Grotenhuis A, Oudega M. Stem cell-based therapies for spinal cord injury. *J Spinal Cord Med*. 2009;32(2):105–114. doi:10.1080/10790268.2009.11760761
13. Cantinieaux D, Quertainmont R, Blacher S, et al. Conditioned medium from bone marrow-derived mesenchymal stem cells improves recovery after spinal cord injury in rats: an original strategy to avoid cell transplantation. *PLoS One*. 2013;8(8):e69515. doi:10.1371/journal.pone.0069515
14. Xie J, MacEwan MR, Schwartz AG, Xia Y. Electrospun nanofibers for neural tissue engineering. *Nanoscale*. 2010;2(1):35–44. doi:10.1039/B9NR00243J
15. Baniasadi H, SA AR, Mashayekhan S. Fabrication and characterization of conductive chitosan/gelatin-based scaffolds for nerve tissue engineering. *Int J Biol Macromol*. 2015;74:360–366. doi:10.1016/j.ijbiomac.2014.12.014
16. Baniasadi H, SA AR, Mashayekhan S, Ghaderinezhad F. Preparation of conductive polyaniline/graphene nanocomposites via in situ emulsion polymerization and product characterization. *Synth Met*. 2014;196:199–205. doi:10.1016/j.synthmet.2014.08.007
17. Vakilian S, Mashayekhan S, Shabani I, Khorashadizadeh M, Fallah A, Soleimani M. Structural stability and sustained release of protein from a multilayer nanofiber/nanoparticle composite. *Int J Biol Macromol*. 2015;75:248–257. doi:10.1016/j.ijbiomac.2015.01.051
18. Moghadasi Boroujeni S, Mashayekhan S, Vakilian S, Ardeshirylajimi A, Soleimani M. The synergistic effect of surface topography and sustained release of TGF-β1 on myogenic differentiation of human mesenchymal stem cells. *J Biomed Mater Res A*. 2016;104(7):1610–1621. doi:10.1002/jbm.a.35686
19. Mashayekhan S, Rasti F. The controlled release of dexamethasone sodium phosphate from bioactive electrospun PCL/gelatin nanofiber scaffold (winter 2019). *Iran J Pharm Res*. 2018.
20. Baron W, Decker L, Colognato H, ffrench-Constant C. Regulation of integrin growth factor interactions in oligodendrocytes by lipid raft microdomains. *Curr Biol*. 2003;13(2):151–155.
21. Popat A, Liu J, Lu GQM, Qiao SZ. A pH-responsive drug delivery system based on chitosan coated mesoporous silica nanoparticles. *J Mater Chem*. 2012;22(22):11173–11178. doi:10.1039/c2jm30501a
22. Ghasemi-Mobarakeh L, Prabhakaran MP, Morshed M, Nasr-Esfahani M-H, Ramakrishna S. Electrospun poly (ε-caprolactone)/gelatin nanofibrous scaffolds for nerve tissue engineering. *Biomaterials*. 2008;29(34):4532–4539. doi:10.1016/j.biomaterials.2008.08.007
23. Cipitria A, Skelton A, Dargaville T, Dalton P, Hutmacher D. Design, fabrication and characterization of PCL electrospun scaffolds—a review. *J Mater Chem*. 2011;21(26):9419–9453. doi:10.1039/c0jm04502k
24. Ghasemi-Mobarakeh L, Prabhakaran MP, Morshed M, Nasr-Esfahani MH, Ramakrishna S. Electrical stimulation of nerve cells using conductive nanofibrous scaffolds for nerve tissue engineering. *Tissue Eng Part A*. 2009;15(11):3605–3619. doi:10.1089/ten.tea.2008.0689
25. Li Y, Li X, Zhao R, et al. Enhanced adhesion and proliferation of human umbilical vein endothelial cells on conductive PANI-PCL fiber scaffold by electrical stimulation. *Mater Sci Eng C*. 2017;72:106–112. doi:10.1016/j.msec.2016.11.052
26. Lee JY, Bashur CA, Goldstein AS, Schmidt CE. Polypyrrole-coated electrospun PLGA nanofibers for neural tissue applications. *Biomaterials*. 2009;30(26):4325–4335. doi:10.1016/j.biomaterials.2009.04.042
27. Rivers TJ, Hudson TW, Schmidt CE. Synthesis of a novel, biodegradable electrically conducting polymer for biomedical applications. *Adv Funct Mater*. 2002;12(1):33–37. doi:10.1002/1616-3028(20020101)12:1<33::AID-ADFM33>3.0.CO;2-E
28. Kim YJ, Kwon OH Crosslinked gelatin nanofibers and their potential for tissue engineering. Paper presented at: Key Engineering Materials; 2007.
29. Broderick EP, O'Halloran DM, Rochev YA, Griffin M, Collighan RJ, Pandit AS. Enzymatic stabilization of gelatin-based scaffolds. *J Biomed Mater Res B Appl Biomater*. 2005;72(1):37–42.
30. Zhang Y, Ouyang H, Lim CT, Ramakrishna S, Huang ZM. Electrospinning of gelatin fibers and gelatin/PCL composite fibrous scaffolds. *J Biomed Mater Res B Appl Biomater*. 2005;72(1):156–165.
31. Soleimani M, Mashayekhan S, Baniasadi H, Ramazani A, Ansarizadeh M. Design and fabrication of conductive nanofibrous scaffolds for neural tissue engineering: process modeling via response surface methodology. *J Biomater Appl*. 2018;33(5):619–629. doi:10.1177/0885328218808917
32. Ko Y-M, Choi D-Y, Jung S-C, Kim B-H. Characteristics of plasma treated electrospun polycaprolactone (PCL) nanofiber scaffold for bone tissue engineering. *J Nanosci Nanotechnol*. 2015;15(1):192–195. doi:10.1166/jnn.2015.8372
33. Kulkarni S, Joshi S, Lokhande C. Facile and efficient route for preparation of nanostructured polyaniline thin films: schematic model for simplest oxidative chemical polymerization. *Chem Eng J*. 2011;166(3):1179–1185. doi:10.1016/j.cej.2010.12.032
34. Jun I, Jeong S, Shin H. The stimulation of myoblast differentiation by electrically conductive sub-micron fibers. *Biomaterials*. 2009;30(11):2038–2047. doi:10.1016/j.biomaterials.2008.12.063
35. Zhang K, Zhang LL, Zhao X, Wu J. Graphene/polyaniline nanofiber composites as supercapacitor electrodes. *Chem Mater*. 2010;22(4):1392–1401. doi:10.1021/cm902876u
36. Kim J, Kim Y-R, Kim Y, et al. Graphene-incorporated chitosan substrata for adhesion and differentiation of human mesenchymal stem cells. *J Mater Chem B*. 2013;1(7):933–938. doi:10.1039/c2tb00274d
37. Li Y-S, Chen B-F, Li X-J, Zhang WK, Tang H-B, Lee M-H. Cytotoxicity of polyaniline nanomaterial on rat celiac macrophages in vitro. *PLoS One*. 2014;9(9):e107361. doi:10.1371/journal.pone.0107361
38. Noriega SE, Hasanova GI, Schneider MJ, Larsen GF, Subramanian A. Effect of fiber diameter on the spreading, proliferation and differentiation of chondrocytes on electrospun chitosan matrices. *Cells Tissues Organs*. 2012;195(3):207–221. doi:10.1159/000325144
39. Fan W, Yan W, Xu Z, Ni H. Formation mechanism of monodisperse, low molecular weight chitosan nanoparticles by ionic gelation technique. *Colloids Surf B Biointerfaces*. 2012;90:21–27. doi:10.1016/j.colsurfb.2011.09.042
40. Okabe N, Mano N, Tahira S. Binding characteristics of a major thyroid hormone metabolite, 3, 3′ 5′-triiodo-L-thyronine, to bovine serum albumin as measured by fluorescence. *Biochim Biophys Acta Gen Subj*. 1989;990(3):303–305. doi:10.1016/S0304-4165(89)80049-2
41. Seidlits SK, Liang J, Bierman RD, et al. Peptide-modified, hyaluronic acid-based hydrogels as a 3D culture platform for neural stem/progenitor cell engineering. *J Biomed Mater Res A*. 2019;107(4):704–718. doi:10.1002/jbm.a.36603
42. Amaral AI, Tavares JM, Sonnewald U, Kotter MRN. Oligodendrocytes: development, physiology and glucose metabolism. In: Schousboe A, Sonnewald U, editors. *The Glutamate/GABA-Glutamine Cycle: Amino Acid Neurotransmitter Homeostasis*. Cham: Springer International Publishing; 2016:275–294.
43. Flores-Obando RE, Freidin MM, Abrams CK. Rapid and specific immunomagnetic isolation of mouse primary oligodendrocytes. *J Vis Exp*. 2018;135:e57543.
44. Shrestha B, Coykendall K, Li Y, Moon A, Priyadarshani P, Yao L. Repair of injured spinal cord using biomaterial scaffolds and stem cells. *Stem Cell Res Ther*. 2014;5(4):91. doi:10.1186/scrt480

45. Darras VM. The role of maternal thyroid hormones in avian embryonic development. *Front Endocrinol (Lausanne)*. 2019;10:66. doi:10.3389/fendo.2019.00066
46. Abbaszadeh H-A, Tiraihi T, Delshad AR, Zadeh MS, Taheri T. Bone marrow stromal cell transdifferentiation into oligodendrocyte-like cells using triiodothyronine as a inducer with expression of platelet-derived growth factor α as a maturity marker. *Iran Biomed J*. 2013;17(2):62.
47. Christopherson GT, Song H, Mao H-Q. The influence of fiber diameter of electrospun substrates on neural stem cell differentiation and proliferation. *Biomaterials*. 2009;30(4):556–564. doi:10.1016/j.biomaterials.2008.10.004